Published in final edited form as:
Biol Psychiatry. 2010 July 1; 68(1): 70–77. doi:10.1016/j.biopsych.2010.03.025.

Corpus Callosum Abnormalities and their Association with Psychotic Symptoms in Patients with Schizophrenia

Thomas J. Whitford, Ph.D.[1,2,*], **Marek Kubicki, M.D., Ph.D.**[1,3], **Jason S. Schneiderman, Ph.D.**[1], **Lauren J. O'Donnell, Ph.D.**[4,5], **Rebecca King, B.Sc.**[1], **Jorge L. Alvarado, B.Sc.**[1], **Usman Khan, B.Sc.**[1], **Douglas Markant, B.Sc.**[1], **Paul G. Nestor, Ph.D.**[3,6], **Margaret Niznikiewicz, Ph.D.**[3], **Robert W. McCarley, M.D., PhD.**[3], **Carl-Fredrik Westin, Ph.D.**[4], and **Martha E. Shenton, Ph.D.**[1,3]

[1]Psychiatry Neuroimaging Laboratory, Department of Psychiatry, Brigham and Women's Hospital, Harvard Medical School, Boston, MA, USA

[2]Melbourne Neuropsychiatry Centre, Department of Psychiatry, University of Melbourne and Melbourne Heath, Melbourne, VIC, Australia

[3]Clinical Neuroscience Division, Laboratory of Neuroscience, Department of Psychiatry, Veterans Affairs (VA) Boston Healthcare System, Harvard Medical School Brockton, MA, USA

[4]Laboratory of Mathematics in Imaging, Brigham and Women's Hospital, Harvard Medical School, Boston, MA, USA

[5]Golby Laboratory, Department of Neurosurgery, Brigham and Women's Hospital, Harvard Medical School, Boston, MA, USA

[6]College of Liberal Arts, University of Massachusetts - Boston, Boston, MA, USA

Abstract

Background—Whilst the neuroanatomical underpinnings of the functional brain disconnectivity observed in patients with schizophrenia remain elusive, white matter fiber bundles of the brain are a likely candidate given that they represent the infrastructure for long-distance neural communication.

Methods—This study investigated for diffusion abnormalities in 19 patients with chronic schizophrenia (SZ), relative to 19 matched controls, across tractography-defined segments of the Corpus Callosum. Diffusion-weighted images were acquired with 51 non-collinear gradients on a 3T scanner (1.7mm isotropic voxels). The Corpus Callosum was extracted by means of whole-brain tractography and automated fiber-clustering, and was parcellated into six segments on the basis of fiber trajectories. The diffusion indices of Fractional Anisotropy (FA) and Mode were calculated for each segment.

Results—Relative to the healthy controls, the SZ patients exhibited Mode increases in the Parietal fibers, suggesting a relative absence of crossing fibers. SZ patients also exhibited FA reductions in the Frontal fibers, which were underpinned by increased in Radial Diffusivity, consistent with myelin abnormalities. Significant correlations were observed between patients' degree of Reality Distortion

* Corresponding Author: Thomas J. Whitford, Psychiatry Neuroimaging Laboratory, Brigham and Women's Hospital, Harvard Medical School, 1249 Boylston St, Boston, MA, 02215, Phone: +1 617 525 1059, Fax: +1 617 525 6150, whitford@bwh.harvard.edu.

Financial Disclosures: None of the authors report having any biomedical financial interests or potential conflicts of interest

and their FA and Radial Diffusivity, such that the most severely psychotic patients were the least abnormal in terms of their Frontal fiber diffusivity.

Conclusions—The SZ patients exhibited a variety of diffusion abnormalities in the Corpus Callosum, which were related to the severity of their psychotic symptoms. To the extent that diffusion abnormalities influence axonal transmission velocities, these results provide support for those theories that emphasize neural timing abnormalities in the etiology of schizophrenia.

Keywords

Schizophrenia; Corpus Callosum; Diffusion Tensor Imaging; Tractography; Fractional Anisotropy; Mode

Introduction

The unifying tenet of the increasingly popular 'disconnectivity' theories of schizophrenia (SZ) (1-3) is that the disorder is ultimately caused by abnormal *interactions* between pathological brain regions, as opposed to regional neuropathology *per se*. In addition to providing a *prima facie* account of the cognitive disorganization characteristic of the disease, support for the 'disconnectivity' theories has been provided by a number of electrophysiological and functional imaging studies that have reported abnormalities in the degree of correlated activity between spatially disparate brain regions in patients with schizophrenia (4-6). The neuroanatomical underpinnings of this aberrant functional connectivity are as yet unknown and represent a point of divergent focus (but not, it should be emphasized, contradiction) between the various 'disconnectivity' theories. Whilst some models have emphasized the role of aberrant synaptic plasticity in the etiology of the disorder (2), others have focused on the role of abnormalities in the physical infrastructure for long-distance neural communication, i.e., white matter (WM) (3). With respect to the latter, white matter is primarily constituted of the phospholipid processes (known as myelin) of a specialized class of neuroglia called oligodendrocytes (7). Myelin ensheaths axons in the nervous system, electrically insulating the axon membrane and increasing the conduction velocity of action potentials. Myelinated axons with similar destinations fasciculate into fiber bundles, which constitute the primary infrastructure for communication between spatially disparate brain regions. It has previously been suggested that abnormalities in WM fiber bundles could represent the neuroanatomical bases for many of the observed abnormalities in functional connectivity in patients with schizophrenia (3).

The Corpus Callosum (CC) is the largest WM fiber bundle in the brain and connects homologous regions of the two cerebral hemispheres. The CC has been implicated in SZ by those who emphasize the role of abnormal hemispheric specialization and abnormal interhemispheric communication in the etiology of the disease (8). Whilst conventional MRI has provided only equivocal evidence for CC abnormalities in patients with schizophrenia (see (9) for a review), a more consistent picture of structural abnormality has been provided by those studies that have employed the more sensitive (at least with respect to WM pathology) modality of Diffusion Tensor Imaging (DTI) (see (10) for a review). However, whilst these previous studies have provided novel and valuable information regarding the location and extent of SZ-specific structural abnormalities in the CC, they have also exhibited some methodological limitations.

Firstly, the majority of previous studies have employed a somewhat arbitrary protocol for segmenting the CC, often based on geometric rather than anatomical boundaries, which may be insufficiently sensitive to detect subtle, regionally-specific diffusion abnormalities. Secondly, most previous DTI studies have investigated for group-wise differences on only a

single diffusivity metric - namely Fractional Anisotropy (FA), which is a measure of the asphericity of water diffusion. However, as noted by Hasan (11), FA is only able to provide a limited picture as to the three-dimensional shape of the observed diffusion. FA cannot, for example, distinguish between prolate (i.e., cigar shaped) and oblate (i.e., pancake shaped) diffusion, despite these presumably having markedly different microstructural underpinnings. The present study aimed to address these methodological limitations in two ways. Firstly, this study employed a previously validated analysis method (12) to distinguish between fiber bundles on the basis of the cortical regions to which they projected, thus avoiding the need for an inflexible geometric schema. Secondly, in addition the stalwart metric of FA, this study also investigated a second, orthogonal diffusion index: Mode (13). Mode is a measure of the prolateness / oblateness of a diffusion ellipsoid, thus providing additional insight into the three-dimensional shape (and hence microstructural underpinnings) of observed diffusion, relative to that provided by FA alone.

The second aim of this study was to investigate the basis for a consistently reported, if somewhat paradoxical finding of a *positive* correlation between SZ patients' FA and the severity of their hallucinations and delusions (14-17). Although the explanation behind this curious relationship has not yet been established, we have recently suggested that while psychotic symptoms may arise when the brain attempts to integrate *mildly* temporally dysmetric activity in spatially disparate cerebral regions, more severe temporal discoordinations might not be able to be integrated and thus might be incapable of giving rise to psychotic symptoms (18). Given the role that WM (and especially myelin) is known to play in modulating the speed of neural transmission, we predicted that severely psychotic SZ patients would show *less* extensive myelin abnormalities relative to SZ patients with less severe psychotic symptoms.

In summary, the two aims of the present study were: 1) to provide a comprehensive description of the shape and extent of water diffusion across tractography-defined subregions of the CC, with the aim of inferring the microstructural underpinnings of any observed diffusion abnormalities in SZ patients, and 2) to investigate the relationship between psychotic symptom severity and WM integrity (as assessed with FA and Radial Diffusivity, the latter of which has been proposed as a putative measure of myelin integrity (19)) in SZ patients.

Methods and Materials

Participants

Nineteen male patients with chronic schizophrenia were recruited from out-patient, in-patient, day treatment and foster care programs at the VA Boston Healthcare System, Brockton, MA. Diagnosis of schizophrenia was made in accordance with DSM-IV criteria on the basis of the Structured Clinical Interview for DSM-IV (conducted by a clinically and research-trained psychologist (PN)), and a review of the medical record. Nineteen male healthy control subjects were recruited from the general community. The control subjects were group matched to the patients on age, handedness, parental socioeconomic status (20), and estimated premorbid IQ, as assessed by performance on the Reading scale of Wide Range Achievement Test (WRAT-3) (21). More than 90% of the participants in this study were new (10% were previously tested on the 1.5T magnet), and none overlapped with the samples described in previous studies by our group (e.g., 22,23,24).

Exclusion criteria for all subjects were left-handedness, a history of electroconvulsive shock therapy, a history of neurological illness including epilepsy, a lifetime history of substance dependence or a history of substance abuse within the past 5 years, a history of steroid use, and estimated premorbid IQ below 75. Furthermore, control subjects were screened for the presence of an Axis-I disorder using the SCID-Non-Patient edition (25), and were also excluded if they reported having first-degree relative with an Axis I disorder.

The study was approved by the VA Boston Healthcare System, the Harvard Medical School Internal Review Board Committee, and the Brigham and Women's Hospital Human Subjects Committee. After a detailed description of the study, each subject gave written informed consent to participate. The demographic details for the patients and controls are summarized in Table 1.

Image Acquisition

Diffusion data were collected on 3 Tesla GE Echospeed system (General Electric Medical Systems, Milwaukee, WI). Diffusion-weighted images (DWIs) were acquired using an echo planar imaging sequence, and a double echo option to reduce eddy-current related distortions. To reduce impact of EPI spatial distortion, an 8 Channel coil and ASSET (Array Spatial Sensitivity Encoding techniques, GE) with a SENSE-factor (speed-up) of 2 was used. Eighty-five axial slices parallel to the AC-PC line covering whole brain were acquired, in 51 diffusion directions with b=900. In addition, 8 baseline scans with b=0 were also acquired. The scan parameters were as follows: TR 17000 ms, TE 78 ms, FOV 24 cm, 144×144 matrix, 1.7 mm slice thickness, producing isotropic 1.7×1.7×1.7mm voxels. The total scanning time was 17 minutes.

Whole-Brain Tractography

The methods used in this study have been described in detail elsewhere (12). For each subject and each image element (voxel), diffusion tensors were estimated from the 59 DWIs. The resultant DTIs were first edited to remove extra-cerebral voxels via a semi-automated generation of a brain ‘mask’. Deterministic (streamline) tractography was then performed via a Runge-Kutta second order protocol with a fixed step size of 0.5mm. Seed-points were placed at every point for which Westin's Linear Anisotropy measure (CL) was greater than 0.3 (the seeding criterion). Tractography proceeded from each seed point in 0.5mm steps, and followed the principal direction of the diffusion ellipsoid. Tracking was stopped when CL fell below 0.15. The seeding and stopping thresholds were based on the CL rather than on FA in order to avoid the circularity inherent in using a dependent variable to define the trajectories of the fiber tracts being measured. A length threshold was also employed whereby fibers were excluded if they were shorter than 20mm.

Fiber Clustering

The fiber-clustering procedure has been described in detail previously (26). The whole-brain tractography procedure (see Fig.1a) generated somewhere in the vicinity of twenty thousand fibers per subject. The purpose of fiber clustering was to group fibers with similar shapes and spatial positions into clusters. Firstly, Fractional Anisotropy (FA) maps calculated for each subject were mapped into a common coordinate system using a congealing registration (27), and the parameters for this registration were applied to each subjects' 3-dimensional set of fiber trajectories. Secondly, each fiber was compared with every other fiber in the trajectory set, and the average distance between pairs of nearest points on the fibers was calculated. This mean fiber-distance (D_{ij}) was then converted into a ‘similarity value’ (W_{ij}) via the formula $W_{ij}=e^{-D_{ij}^2/\theta^2}$, where θ = 60mm. The role of θ was to set the distance over which fibers could be considered similar (26). The ‘similarity value’ of each fiber to every other fiber was entered into an ‘affinity matrix’ (W), and the top 15 eigenvectors of W were used to calculate the most important shape similarity information for each fiber. The clustering algorithm used k-way normalized cuts, which produces clusters with high within-cluster similarity and low between-cluster similarity (28). Fiber clustering was performed on the amalgamated fiber tracts of all subjects in the study (as opposed to clustering each subject separately), as this enabled the identification of homologous fiber-clusters (FCs) between subjects. Tractography and fiber

clustering were performed using Matlab 7.0 (www.mathworks.com) and 3D-Slicer (www.slicer.org), which is freely available to the research community.

Extraction and Segmentation of the Corpus Callosum

The output of the clustering procedure was 400 FCs, each consisting of a spatially and morphologically similar subset of the fibers generated from the whole-brain tractography (see Fig.1b). Of these 400 FCs, 75 were judged to constitute the Corpus Callosum, based on the consensus of two independent raters (TW and JS) on three randomly-selected participants (inter-rater reliability = 0.901). These 75 Corpus FCs were automatically extracted from all participants (on the basis of their unique cluster labels (29)), and the validity of these extracted FCs confirmed by a third rater (MK). These CC FCs were then subdivided into six segments on the basis of the cortical regions to which they projected (see Fig.1c). Using these cluster labels, the FCs constituting the CC were automatically extracted for each subject, and subsequently subdivided into six segments on the basis of the cortical regions to which they projected. The six segments, which are described and illustrated in Fig.1d, were: Frontal fibers (CC1), Premotor fibers (CC2), Sensorimotor fibers (CC3), Parietal fibers (CC4), Occipital fibers (CC5) and Temporal fibers (CC6).

Diffusion Indices

Fractional Anisotropy (FA) and Mode were calculated at every voxel for each subject.

Mode is an index of the 3-dimensional shape of diffusion - specifically whether it is better described by an oblate (shaped like a pancake; Mode ≈ -1) or prolate (shaped like a cigar; Mode ≈ 1) ellipsoid.

$$\text{Mode}=\frac{(2\lambda_1-\lambda_2-\lambda_3)(\lambda_1-2\lambda_2+\lambda_3)(\lambda_1+\lambda_2-2\lambda_3)}{2(\sqrt{\lambda_1\lambda_1+\lambda_2\lambda_2+\lambda_3\lambda_3-\lambda_1\lambda_2-\lambda_2\lambda_3-\lambda_1\lambda_3})^3}$$

Fractional Anisotropy (FA) is an index of the asphericity of diffusion, and is calculated as:

$$\text{FA}=\frac{\sqrt{(\lambda_1-\lambda_2)^2+(\lambda_2-\lambda_3)^2+(\lambda_1-\lambda_3)^2}}{\sqrt{2}\sqrt{\lambda_1^2+\lambda_2^2+\lambda_3^2}}$$

Mean values of the diffusivity indices were calculated for each CC segment, for each subject. This was done by averaging the diffusivity values (i.e., FA and Mode) of all voxels through which passed any of the FCs that constituted a given CC segment.

In order to help further infer the microstructural underpinnings of any abnormalities in FA, two additional diffusion indices were calculated for only those segments for which group-wise differences in FA were observed. These two indices – namely Radial Diffusivity and Axial Diffusivity – have been proposed as being sensitive to abnormalities in myelination (19,30) and axon integrity (31), respectively. Radial Diffusivity is a measure of the extent of diffusion perpendicular to the principal axis of the diffusion ellipsoid, and is calculated as: $\frac{\lambda_2+\lambda_3}{2}$. Axial Diffusivity is a measure of the absolute extent of diffusion along the principal axis of the diffusion ellipsoid, and is calculated as: λ_1

Statistical Analysis

The statistical analysis was performed using SPSS v11 (www.spss.com). Given the confounds associated with using a Repeated-Measures design in the context of severe violations of sphericity (32), a Multivariate Analysis of Variance (MANOVA) was used to identify between-group differences in FA and Mode. To control for multiple comparisons, Fisher's Protected Test was employed (33). If (and only if) the MANOVA identified an overall between-group difference in a diffusion index were *post hoc* contrasts (Fisher's LSD) used to identify the CC segments responsible for the omnibus effect.

Pearson's partial correlations (controlling for CPZ-equivalent medication dosage) were used to investigate the relationship between patients' FA and Radial Diffusivity and their Reality Distortion symptom score. As per Liddle (34), Reality Distortion was calculated for each patient as the sum of their scores on the Hallucination and Delusion subscales of the Positive and Negative Symptom Scale (PANSS). Correlations between FA / Radial Diffusivity and patients' scores on the PANSS-Negative and PANSS-General subscales were also investigated. In order to limit the number of statistical comparisons, these correlations were only investigated for those CC segments which were identified as being abnormal in the patient group.

Results

Figure 2 shows the scatterplots for FA (Fig.2a) and Mode (Fig.2b) across the 6 CC segments, for the SZ (red) and Control (blue) groups.

Multivariate ANOVA revealed significant between-group differences in FA ($F(6,31)=3.537$, $p=0.009$). *Post hoc* analysis revealed that the FA of CC1 (i.e., the Frontal fibers) was significantly decreased in the SZ patients relative to controls ($t(1,36)=2.282$ $p=0.029$). Additional analyses were performed in order to determine whether the FA reductions in CC1 were underpinned by changes in Axial or Radial Diffusivity. The SZ patients exhibited significant increases in Radial Diffusivity in CC1 ($t(1,36)=2.218$, $p=0.033$), but no differences in Axial Diffusivity ($t(1,36)=0.113$, $p=0.911$), relative to controls (Fig.3).

Significant between-group differences in Mode were also observed ($F(6,31)=2.417$, $p=0.049$) (Fig.2b). *Post hoc* analysis revealed that Mode was significantly increased (indicating a more cigar-shaped diffusion ellipsoid) in CC4 (i.e., the Parietal fibers) in the SZ patients relative to controls ($t(1,36)=2.291$, $p=0.028$).

Significant positive correlations (controlling for patients' CPZ-equivalent medication dosage) were observed between FA in CC1 and SZ patients' Reality Distortion scores ($r(16)=.601$, $p=0.008$) (Fig.4a). Conversely, significant negative correlations were observed between Radial Diffusivity in CC1 and SZ patients' Reality Distortion scores ($r(16)=-.538$, $p=0.021$) (Fig.4b). The results of these correlations were similar (and remained statistically significant) when CPZ-equivalent medication dosage was removed as a covariate.

There was a (non-significant) trend for a *negative* correlation between patients' FA in CC1 and their total score on the PANSS-Negative subscale, controlling for medication dosage ($r(16)=-.341$, $p=0.166$). Each of the individual PANSS-Negative items was found to be negatively correlated with FA in CC1, although this only reached statistical significance for item N5 (difficulty in abstract thinking) ($r(16)=-.477$, $p=0.046$). No statistically significant correlations were observed between patients' FA in CC1 and their scores on the PANSS-General scale or subscales.

No significant correlations were observed between patients' CPZ-equivalent medication dosage and their FA or Mode in any of the six CC segments (see Supplement 1). In contrast,

significant negative correlations were observed between age and FA across groups, consistent with several previous studies (35-37) (see Supplement 1).

Discussion

The primary findings of this study were of FA and Radial Diffusivity abnormalities in the Frontal CC fibers, and Mode abnormalities in the Parietal CC fibers in 19 SZ patients relative to 19 matched healthy controls. Furthermore, the severity of patients' symptoms of Reality Distortion (i.e., hallucinations and delusions) were found to be positively correlated with FA and negatively correlated with Radial Diffusivity in the Frontal CC fibers. In light of the FA reductions and Radial Diffusivity increases which were observed in the SZ patients in this CC segment, these results suggest that the most severely psychotic patients were the least abnormal in terms of their FA and Radial Diffusivity in these fibers.

Whilst FA reductions in the genu of the CC in SZ patients have been reported previously (38,39), including in patients with first-episode SZ (40) (see (10,41) for reviews), their microstructural underpinnings have not been well established. FA reductions have been found to occur in response to axon death, myelin damage, damage to the axon membrane, and reduced 'fiber coherence' (i.e., more variable fiber trajectories within a WM bundle) (10,42). While there is little evidence to suggest the presence of any substantial degree of abnormal neuron death in SZ patients (e.g., see (43)), there is, in contrast, a growing body of evidence suggesting that SZ patients exhibit abnormalities in both their myelin and in the integrity of their axon membranes (44,45). Distinguishing between these two distinct neuropathologies was one motivation behind the development of the diffusion indices Axial and Radial Diffusivity. In a series of animal studies, Song (19) demonstrated that while damage to the myelin of the optic nerve resulted in increased Radial (but unchanged Axial) Diffusivity, damage to the axonal membrane of the optic nerve (but preservation of the myelin) resulted in reduced Axial but unchanged Radial Diffusivity (31). The results of these studies support the claim that Radial Diffusivity is a putative measure of myelin integrity while Axial Diffusivity is a putative measure of axonal integrity. Hence the results of the present study in which the SZ patients were observed to exhibit abnormally increased Radial Diffusivity but unchanged Axial Diffusivity, relative to controls, in the Frontal CC fibers, suggests that the FA abnormalities in these fibers were more likely underpinned by myelin abnormalities as opposed to damage to the axon membrane.

If the observed diffusion abnormalities in the Frontal CC fibers were indeed the result of myelin damage, then this might be expected to result in slowed impulse conduction (46). Furthermore, it might also seem likely that those SZ patients with the most profound diffusion abnormalities (and hence presumably the most severe conduction delays) would exhibit the most severe psychopathology. Such a relationship, however, was not observed in the present study. On the contrary, those SZ patients with the most subnormal levels of FA (and most supranormal levels of Radial Diffusivity) exhibited the *least* severe symptoms of Reality Distortion. Far from being an unprecedented finding, this seemingly paradoxical result of a *positive* correlation between FA and psychotic symptom severity has been reported many times previously, including in the CC (17,47), cingulum bundle (17), arcuate fasciculus (17), superior longitudinal fasciculus (14,15) and inferior fronto-occipital fasciculus (16). It was also notable that, in the present study, the most severely psychotic patients did not show *abnormally* high levels of FA, but instead exhibited FA values lower than the healthy controls but higher than the less-psychotic patients (see Fig.4). What is the explanation for this seemingly paradoxical finding that the more floridly psychotic a SZ patient, the less severe their FA abnormalities?

To the extent that axonal conduction delays can be inferred from diffusivity abnormalities in DTI, these results suggest that while some amount of neural desynchronization may be

necessary for the development of psychotic symptoms, too much desynchronization may in fact preclude the development of highly systematized hallucinations and delusions such as would score highly on a clinical rating scale such as the PANSS. This idea has some support in the WM literature. For example, while psychotic symptoms have been commonly reported in patients with the degenerative demyelinating disease metachromatic leukodystrophy (48), they are more likely to occur in the early stages of the disease when myelin pathologies are relatively minor compared to the late stages of the disease when severe demyelination is apparent (49). If it is true that psychotic symptoms represent the brain's attempt to incorporate disjointed neural activity into a coherent (albeit pathological) framework (50), then perhaps this “pathological integration” is only possible up to a certain level of temporal desynchronization. In other words, while mild asynchronies between the activities of spatially discrete brain regions might give rise to psychotic symptoms (such as, for example, between the different brain regions stimulated by a primary discharge and its corollaries (51)), severe asynchronies (such as might be caused by severe WM damage) might not be incorporable into a coherent phenomenological framework and thus not give rise to psychotic symptoms. Such severe WM damage could instead result in something of a ‘cognitive shutdown’ which could underlie the negative symptoms of SZ. This would explain the *negative* correlation between FA and negative symptom severity that has been observed previously in SZ patients (16,47, 52), and for which there was a non-significant trend in the present study. Testing these hypotheses could potentially provide a fruitful avenue for future research.

Our finding of abnormally increased Mode (i.e., abnormally prolate diffusion ellipsoids) in the Parietal CC fibers in the SZ patients has not (to our knowledge) been reported previously. Mode is a relatively recently-developed measure which provides independent and complementary information to the stalwart index of FA (13). In terms of its physiological determinants, Mode has been found to decrease in the presence of fiber crossings (13). Thus one explanation as to why the SZ patients exhibited abnormally increased Mode but normal levels of FA in the parietal CC fibers might be that the patients evince abnormalities in a fiber bundle adjacent to these CC fibers (e.g., the cingulum bundle, as recently suggested by Mandah et al., (53)), resulting in a reduction in the density of fiber crossings, and hence elevated Mode, in this region of the CC. Our finding of diffusion abnormalities in the Parietal CC fibers is also consistent with the results of several early-onset studies which have reported parietal lobe white matter to be among the first cerebral areas to evince structural abnormalities in patients with schizophrenia – abnormalities that have been argued to contribute to the emergence of psychotic symptoms through their effects on frontal-parietal connectivity (54,55).

A limitation of the present study relates to the fact that all of the SZ patients were suffering from chronic schizophrenia and had been at least intermittently (and in many cases chronically) exposed to neuroleptic medications. This is relevant in light of evidence from primate studies suggesting that exposure to both typical and atypical neuroleptics can influence brain structure in and of itself (56). Notwithstanding the fact that a) patients' chlorpromazine-equivalent medication dosages were statistically controlled for in the present study, and b) there were no significant correlations between patients' CPZ-equivalent medication dosages and their FA, Mode, or Radial Diffusivity in any of the 6 CC segments (see Supplement 1), replicating these results in a population of first-episode, neuroleptic-naive SZ patients would strengthen confidence into their validity, and would be a worthwhile aim for future research. A second limitation relates to the fact that all the patients were male. Whilst this was advantageous in the sense that it increased the homogeneity of the sample and thus the power, it obviously limited the extent to which the results can be generalized to females.

In summary, the main findings of this study were of FA reductions and Radial Diffusivity increases in Frontal CC fibers (consistent with dysmyelination) and Mode increases in Parietal CC fibers (consistent with a relative absence of crossing fibers) in 19 patients with

schizophrenia relative to 19 matched healthy controls. Significant correlations were also observed between patients' FA and Radial Diffusivity in the Frontal fibers and the severity of their psychotic symptoms, such that patients with the *most* abnormal levels of FA and Radial Diffusivity exhibited the *least* severe symptoms of Reality Distortion. This result, we suggest, provides support for those theories which emphasize neural timing abnormalities in the etiology of psychotic symptoms.

Supplementary Material

Refer to Web version on PubMed Central for supplementary material.

Acknowledgments

Thomas Whitford is supported by an Overseas-Based Biomedical Training Fellowship from the National Health and Medical Research Council of Australia (NHMRC 520627), administered through the University of Melbourne. Marek Kubicki is supported by grants from the National Institutes of Health (R03 MH068464-0; R01 MH 50747 to MES), the Harvard Medical School (Milton Award), and the National Alliance for Research on Schizophrenia and Depression. Jason Schneiderman is supported by a fellowship from the National Institutes of Health (T32 MH 016259). Martha Shenton is supported by grants from the National Institutes of Health (K05 MH 070047 and R01 MH 50747), the Department of Veterans Affairs (VA Merit Award, VA Research Enhancement Award Program and VA Schizophrenia Research Center Grant), and the Boston Center for Intervention Development and Applied Research (CIDAR) funded through a center grant mechanism (P50 MH 080272). Robert McCarley is supported by grants from the Department of Veterans Affairs (VA Merit Award, VA Schizophrenia Research Center Grant), the National Institute of Mental Health (MH 040799), and the Boston Center for Intervention Development and Applied Research (CIDAR, P50 MH 080272). Lauren O'Donnell is supported by an R25 grant from the National Institute of Health (CA089017-06A2). This work is also supported, in part, from the National Alliance for Medical Image Computing (NAMIC), funded by the National Institutes of Health through the NIH Roadmap Initiative for Medical Research (Grant U54 EB005149 to Kubicki and Shenton). All authors listed contributed to the study by either being involved in the design and implementation (TW, MK, MES, JSS), the methodology used (TW, MK, MES, LO, CFW), the data acquisition and analysis (TW, MK, RK, JLA, UK, DM, MN, PN), the interpretation of neuropsychological measures (PN), or were involved in the writing (TW, MK, MES, JSS, LO, MN, RWM).

References

1. Andreasen NC. A unitary model of schizophrenia: Bleuler's “fragmented phrene” as schizencephaly. Archives of General Psychiatry 1999;56:781–787. [PubMed: 12884883]
2. Friston K. Schizophrenia and the disconnection hypothesis. Acta Psychiatr Scand Suppl 1999;395:68–79. [PubMed: 10225335]
3. Bartzokis G. Schizophrenia: breakdown in the well-regulated lifelong process of brain development and maturation. Neuropsychopharmacology 2002;27:672–683. [PubMed: 12377404]
4. Norman RM, Malla AK, Williamson PC, Morrison-Stewart SL, Helmes E, Cortese L. EEG coherence and syndromes in schizophrenia. Br J Psychiatry 1997;170:411–415. [PubMed: 9307688]
5. Fletcher P, McKenna PJ, Friston KJ, Frith CD, Dolan RJ. Abnormal cingulate modulation of fronto-temporal connectivity in schizophrenia. Neuroimage 1999;9:337–342. [PubMed: 10075903]
6. Ragland J, Gur R, Valdez J, Turetsky B, Elliott M, Kohler C, et al. Event-related fMRI of frontotemporal activity during word encoding and recognition in schizophrenia. Am J Psychiatry 2004;161:1004–1015. [PubMed: 15169688]
7. Fields R. The other half of the brain. Sci Am 2004;290:54–61. [PubMed: 15045754]
8. Crow T. Schizophrenia as a transcallosal misconnection syndrome. Schizophr Res 1998;30:111–114. [PubMed: 9549773]
9. Shenton M, Dickey C, Frumin M, McCarley R. A review of MRI findings in schizophrenia. Schizophr Res 2001;49:1–52. [PubMed: 11343862]
10. Kubicki M, McCarley R, Westin CF, Park HJ, Maier S, Kikinis R, et al. A review of diffusion tensor imaging studies in schizophrenia. J Psychiatr Res 2007;41:15–30. [PubMed: 16023676]
11. Hasan K. Diffusion tensor eigenvalues or both mean diffusivity and fractional anisotropy are required in quantitative clinical diffusion tensor MR reports: fractional anisotropy alone is not sufficient. Radiology 2006;239:611–612. author reply 612-613. [PubMed: 16641362]

12. Voineskos A, O'Donnell L, Lobaugh N, Markant D, Ameis S, Niethammer M, et al. Quantitative examination of a novel clustering method using magnetic resonance diffusion tensor tractography. Neuroimage 2009;45:370–376. [PubMed: 19159690]
13. Kindlmann G, Ennis D, Whitaker R, Westin C. Diffusion tensor analysis with invariant gradients and rotation tangents. IEEE Trans Med Imaging 2007;26:1483–1499. [PubMed: 18041264]
14. Shergill S, Kanaan R, Chitnis X, O'Daly O, Jones D, Frangou S, et al. A diffusion tensor imaging study of fasciculi in schizophrenia. Am J Psychiatry 2007;164:467–473. [PubMed: 17329472]
15. Seok J, Park H, Chun J, Lee S, Cho H, Kwon J, et al. White matter abnormalities associated with auditory hallucinations in schizophrenia: a combined study of voxel-based analyses of diffusion tensor imaging and structural magnetic resonance imaging. Psychiatry Res 2007;156:93–104. [PubMed: 17884391]
16. Szeszko P, Robinson D, Ashtari M, Vogel J, Betensky J, Sevy S, et al. Clinical and neuropsychological correlates of white matter abnormalities in recent onset schizophrenia. Neuropsychopharmacology 2008;33:976–984. [PubMed: 17581532]
17. Hubl D, Koenig T, Strik W, Federspiel A, Kreis R, Boesch C, et al. Pathways that make voices: white matter changes in auditory hallucinations. Arch Gen Psychiatry 2004;61:658–668. [PubMed: 15237078]
18. Whitford, TJ.; Kubicki, M.; Shenton, ME. The neuroanatomical underpinnings of schizophrenia and their implications as to the cause of the disorder: a review of the structural MR and diffusion literature. In: Shenton, ME.; Turetsky, B., editors. Neuropsychiatric Imaging. New York: Cambridge University Press; in press
19. Song S, Sun S, Ramsbottom M, Chang C, Russell J, Cross A. Dysmyelination revealed through MRI as increased radial (but unchanged axial) diffusion of water. Neuroimage 2002;17:1429–1436. [PubMed: 12414282]
20. Hollingshead, A. Two factor of index of social position. New Haven: Yale Station; 1965.
21. Wilkinson, GS.; Wide Range, I. The Wide Range Achievement Test - Administration Manual. Wilmingham: Wide Range Inc; 1993.
22. Kubicki M, Westin C, Nestor P, Wible C, Frumin M, Maier S, et al. Cingulate fasciculus integrity disruption in schizophrenia: a magnetic resonance diffusion tensor imaging study. Biol Psychiatry 2003;54:1171–1180. [PubMed: 14643084]
23. Kubicki M, Park H, Westin C, Nestor P, Mulkern R, Maier S, et al. DTI and MTR abnormalities in schizophrenia: analysis of white matter integrity. Neuroimage 2005;26:1109–1118. [PubMed: 15878290]
24. Kubicki M, Styner M, Bouix S, Gerig G, Markant D, Smith K, et al. Reduced interhemispheric connectivity in schizophrenia-tractography based segmentation of the corpus callosum. Schizophr Res 2008;106:125–131. [PubMed: 18829262]
25. First, MB.; Spitzer, RL.; Gibbon, M.; Williams, BJ. Structured Clinical Interview for DSM-IV-TR Axis I Disorders, Research Version, Non-patient Edition (SCID-I/NP). New York: Biometrics Research, New York State Psychiatric Institute; 2002.
26. O'Donnell LJ, Kubicki M, Shenton ME, Dreusicke MH, Grimson WE, Westin CF. A method for clustering white matter fiber tracts. AJNR Am J Neuroradiol 2006;27:1032–1036. [PubMed: 16687538]
27. Zollei L, Learned-Miller E, Grimson E, Wells W. Efficient population registration of 3D data. International Conference of Computer Vision. 2005
28. Ng, A.; Jordan, M.; Weiss, Y. On spectral clustering: analysis and an algorithm. Cambridge, MA: MIT Press; 2002.
29. O'Donnell L, Westin C. White matter tract clustering and correspondence in populations. Med Image Comput Comput Assist Interv 2005;8:140–147. [PubMed: 16685839]
30. Seal M, Yücel M, Fornito A, Wood S, Harrison B, Walterfang M, et al. Abnormal white matter microstructure in schizophrenia: a voxelwise analysis of axial and radial diffusivity. Schizophr Res 2008;101:106–110. [PubMed: 18262770]
31. Song S, Sun S, Ju W, Lin S, Cross A, Neufeld A. Diffusion tensor imaging detects and differentiates axon and myelin degeneration in mouse optic nerve after retinal ischemia. Neuroimage 2003;20:1714–1722. [PubMed: 14642481]

32. Field, A. Discovering Statistics using SPSS. 3. Thousand Oaks, CA: Sage Publications; 2009.
33. Fisher, RA. The design of experiments. Edinburgh: Oliver and Boyd; 1935.
34. Liddle PF. The symptoms of chronic schizophrenia: a re-examination of the positive-negative dichotamy. British Journal of Psychiatry 1987;151:145–151. [PubMed: 3690102]
35. Burzynska A, Preuschhof C, Bäckman L, Nyberg L, Li S, Lindenberger U, et al. Age-related differences in white matter microstructure: Region-specific patterns of diffusivity. Neuroimage 2010;49:2104–2112. [PubMed: 19782758]
36. Zhang Y, AT D, Hayasaka S, Jahng G, Hlavin J, Zhan W, et al. Patterns of age-related water diffusion changes in the human brain by concordance and discordance analysis. Neurobiol Aging. in press.
37. Rosenberger G, Kubicki M, Nestor P, Connor E, Bushell G, Markant D, et al. Age-related deficits in fronto-temporal connections in schizophrenia: a diffusion tensor imaging study. Schizophr Res 2008;102:181–188. [PubMed: 18504117]
38. Buchsbaum M, Friedman J, Buchsbaum B, Chu K, Hazlett E, Newmark R, et al. Diffusion tensor imaging in schizophrenia. Biol Psychiatry 2006;60:1181–1187. [PubMed: 16893533]
39. Kanaan R, Shergill S, Barker G, Catani M, Ng V, Howard R, et al. Tract-specific anisotropy measurements in diffusion tensor imaging. Psychiatry Res 2006;146:73–82. [PubMed: 16376059]
40. Price G, Cercignani M, Parker G, Altmann D, Barnes T, Barker G, et al. Abnormal brain connectivity in first-episode psychosis: a diffusion MRI tractography study of the corpus callosum. Neuroimage 2007;35:458–466. [PubMed: 17275337]
41. Kanaan R, Kim J, Kaufmann W, Pearlson G, Barker G, McGuire P. Diffusion tensor imaging in schizophrenia. Biol Psychiatry 2005;58:921–929. [PubMed: 16043134]
42. Beaulieu C. The basis of anisotropic water diffusion in the nervous system - a technical review. NMR Biomed 15:435–455. [PubMed: 12489094]
43. Pakkenberg B. Total nerve cell number in neocortex in chronic schizophrenics and controls estimated using optical disectors. Biol Psychiatry 1993;34:768–772. [PubMed: 8292680]
44. Uranova N, Vostrikov V, Vikhreva O, Zimina I, Kolomeets N, Orlovskaya D. The role of oligodendrocyte pathology in schizophrenia. Int J Neuropsychopharmacol 2007;10:537–545. [PubMed: 17313698]
45. Davis KL, Stewart DG, Friedman JI, Buchsbaum M, Harvey PD, Hof PR, et al. White matter changes in schizophrenia: evidence for myelin-related dysfunction. Arch Gen Psychiatry 2003;60:443–456. [PubMed: 12742865]
46. Roy K, Murtie J, El-Khodor B, Edgar N, Sardi S, Hooks B, et al. Loss of erbB signaling in oligodendrocytes alters myelin and dopaminergic function, a potential mechanism for neuropsychiatric disorders. Proc Natl Acad Sci U S A 2007;104:8131–8136. [PubMed: 17483467]
47. Rotarska-Jagiela A, Schönmeyer R, Oertel V, Haenschel C, Vogeley K, Linden D. The corpus callosum in schizophrenia-volume and connectivity changes affect specific regions. Neuroimage 2008;39:1522–1532. [PubMed: 18096406]
48. Black D, Taber K, Hurley R. Metachromatic leukodystrophy: a model for the study of psychosis. J Neuropsychiatry Clin Neurosci 2003;15:289–293. [PubMed: 12928504]
49. Weinberger, DR.; Marceno, S. Schizohprenia as a neurodevelopmental disorder. In: Hirsch, SR.; Weinberger, DR., editors. Schizophrenia. 2. New York: Wiley-Blackwell; 2003. p. 326-348.
50. Maher B. Delusional thinking and perceptual disorder. Journal of Individual Psychology 1974;30:98–113. [PubMed: 4857199]
51. Ford J, Gray M, Faustman W, Roach B, Mathalon D. Dissecting corollary discharge dysfunction in schizophrenia. Psychophysiology 2007;44:522–529. [PubMed: 17565658]
52. Wolkin A, Choi S, Szilagyi S, Sanfilipo M, Rotrosen J, Lim K. Inferior frontal white matter anisotropy and negative symptoms of schizophrenia: a diffusion tensor imaging study. Am J Psychiatry 2003;160:572–574. [PubMed: 12611842]
53. Maddah M, Kubicki M, Wells W, Westin C, Shenton M, Grimson W. Findings in schizophrenia by tract-oriented DT-MRI analysis. Medical Image Computing and Computer Assisted Intervention 2008:917–924. [PubMed: 18979833]
54. Kyriakopoulos M, Vyas N, Barker G, Chitnis X, Frangou S. A diffusion tensor imaging study of white matter in early-onset schizophrenia. Biol Psychiatry 2008;63:519–523. [PubMed: 17662964]

55. Kyriakopoulos M, Perez-Iglesias R, Woolley J, Kanaan R, Vyas N, Barker G, et al. Effect of age at onset of schizophrenia on white matter abnormalities. Br J Psychiatry 2009;195:346–353. [PubMed: 19794204]

56. Konopaske G, Dorph-Petersen K, Sweet R, Pierri J, Zhang W, Sampson A, et al. Effect of chronic antipsychotic exposure on astrocyte and oligodendrocyte numbers in macaque monkeys. Biol Psychiatry 2008;63:759–765. [PubMed: 17945195]

57. Rey M, Schulz P, Costa C, Dick P, Tissot R. Guidelines for the dosage of neuroleptics. I: Chlorpromazine equivalents of orally administered neuroleptics. Int Clin Psychopharmacol 1989;4:95–104. [PubMed: 2568378]

58. Woods S. Chlorpromazine equivalent doses for the newer atypical antipsychotics. J Clin Psychiatry 2003;64:663–667. [PubMed: 12823080]

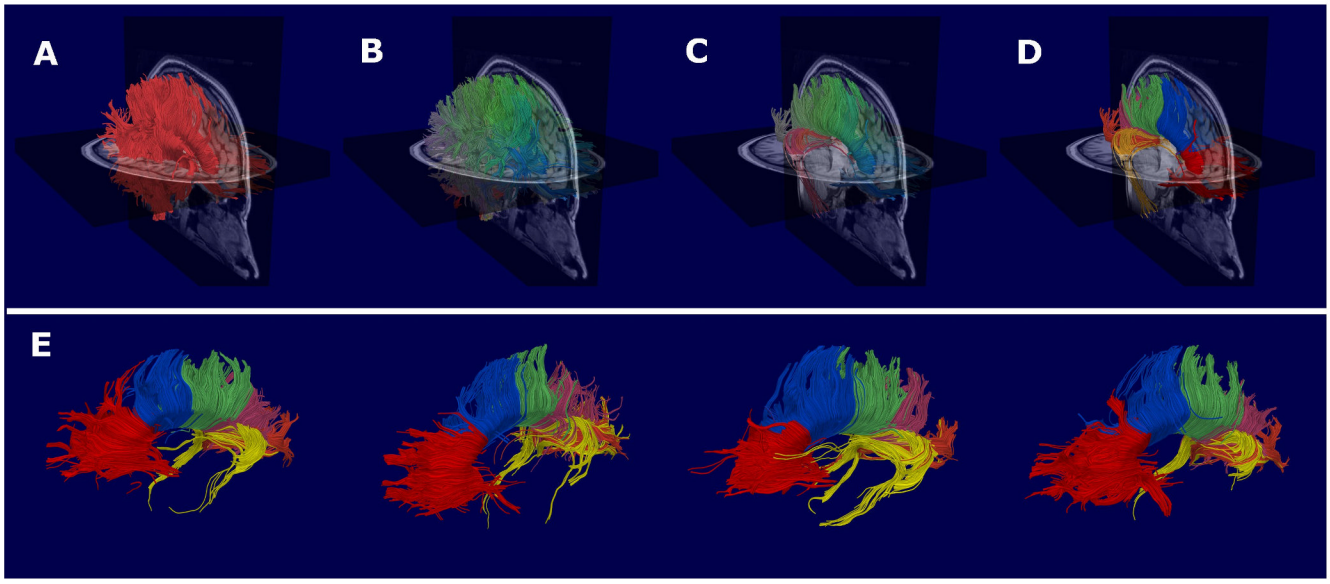

Figure 1.

A summary of the image processing procedures. Firstly, whole-brain tractography was performed on each subject's Diffusion-Weighted Image (Panel A), and the resultant fibers combined for all subjects. Fibers with similar shapes and spatial positions were then grouped together into one of 400 fiber-clusters (Panel B). The fiber-clusters constituting the Corpus Callosum were then identified for a randomly selected subject (Panel C), and subsequently subdivided into six segments on the basis of which cortical regions the fiber-clusters projected (Panel D). The fiber-clusters constituting each of the six Corpus segments were then automatically extracted for all subjects, and the average FA and Mode of these fiber-clusters calculated. As illustrated in Panel D, the six Corpus segments were: CC1 (red) – Frontal fibers (defined as fibers projecting anterior to the SMA), CC2 (blue) – Premotor fibers (defined as fibers projecting to the SMA or premotor areas), CC3 (green) – Sensorimotor fibers (defined as fibers projecting to the primary motor or primary sensory cortices), CC4 (pink) – Parietal fibers (defined as fibers projecting to the superior or inferior parietal lobules), CC5 (orange) – Occipital fibers (defined as fibers projecting posterior to the parieto-occipital sulcus) and CC6 (yellow) – Temporal fibers (defined as fibers projecting ventrally to the temporal cortices). The Corpus segmentations of four randomly selected subjects are displayed in Panel E.

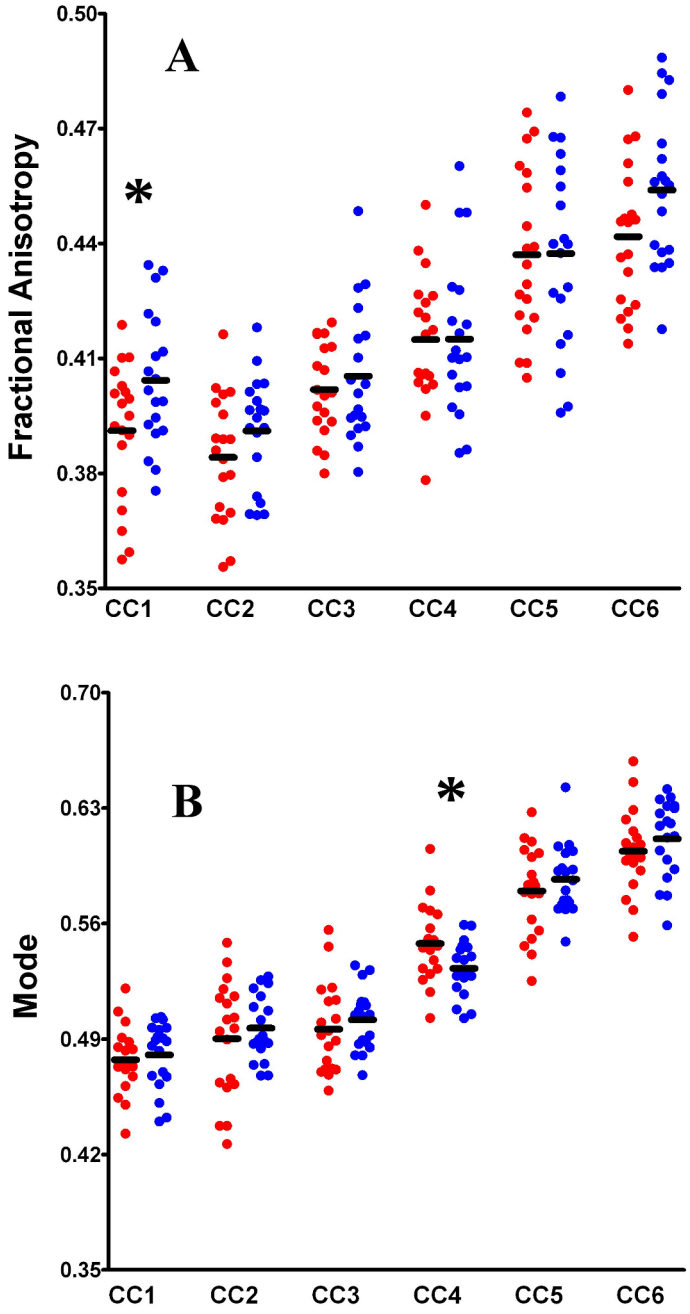

Figure 2.
Scatterplots illustrating the variations in FA (Panel A) and Mode (Panel B), between groups (SZ in red, Controls in blue), and across Corpus segments (CC1 through CC6). The black bars represent CC segment means, and the asterisks represent significant between-group differences in diffusivity.

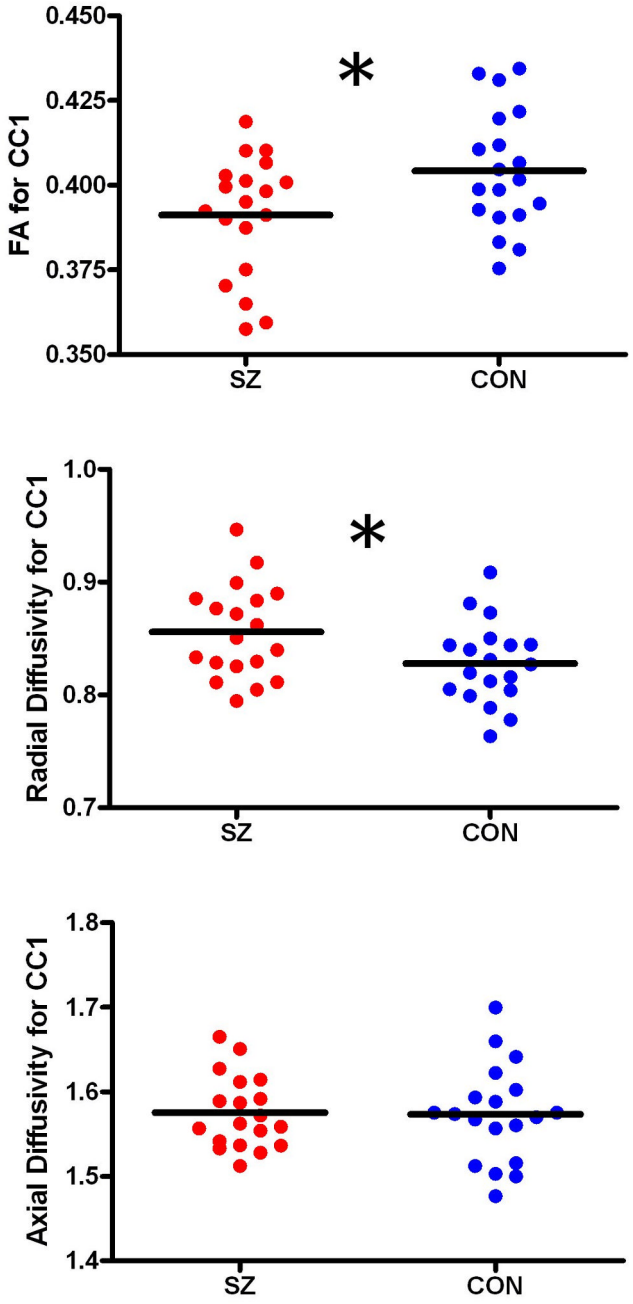

Figure 3.
Scatterplots illustrating the variations in FA (Panel A), Radial Diffusivity (Panel B) and Axial Diffusivity (Panel C) between groups (SZ in red, Controls in blue) for CC1 (frontal fibers). The black bars represent CC segment means, and the asterisks represent significant between-group differences in diffusivity.

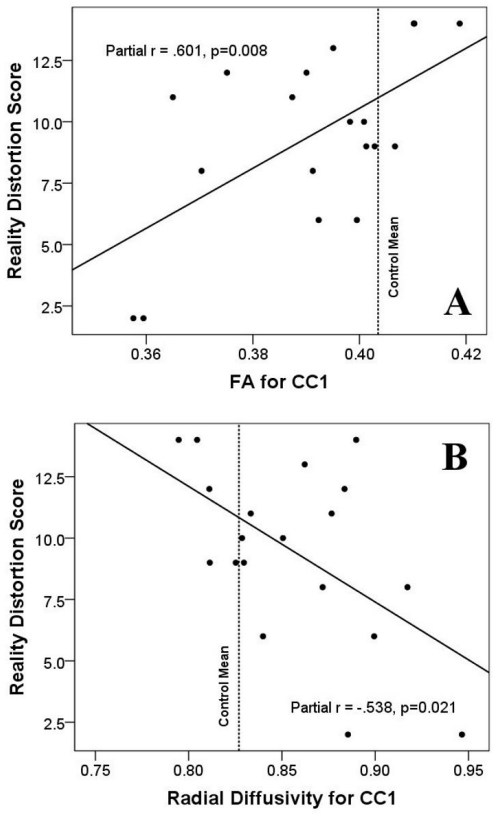

Figure 4.

Scatterplots illustrating the relationships between SZ patients' Reality Distortion score (i.e., the sum of the PANSS-Hallucinations and Delusions subscales) and their FA (Panel A) and Radial Diffusivity (Panel B) in CC1. The black lines represent the line-of-best-linear-fit for the data. The red dotted lines show the mean values of FA and Radial Diffusivity exhibited by the healthy controls.

Table 1

Demographic details of the subject sample – means and standard deviations are provided.

Variable	SZ patients (n=19)	Controls (n=19)	SZ vs. Controls
Age (yrs)	37.9 (9.60)	37.0 (12.2)	t(36)=0.27, p=0.79
Handedness (1=RH, -1=LH)	0.71 (0.25)	0.79 (0.15)	t(30)=0.98, p=0.33
Parental SES	2.63 (1.07)	2.22 (1.16)	t(35)=1.12, p=0.27
Premorbid IQ (WRAT-3 Reading)	94.8 (11.4)	102.4 (9.9)	t(26)=1.80, p=0.08
Medication dosage (CPZ equivalent[1])	334 (288)	-	-
Medication type[2]	2 typical, 13 atypical, 1 both, 3 unmedicated	-	-
Age-at-onset (yrs)	23.5 (5.71)	-	-
PANSS-Positive	22.4 (8.76)	-	-
PANSS-Negative	21.9 (10.4)	-	-
PANSS-General	43.8 (15.5)	-	-

[1]Medication dosages: Patients' medication dosages at time of clinical interview were converted into chlorpromazine (CPZ) equivalents on the basis of the Rey et al. (57) conversion for typical antipsychotics and the Woods (58) conversion for atypical antipsychotics.

[2]Medication type: At the time of interview, two patients were taking typical antipsychotic medications (fluphenazine or haloperidol), thirteen were taking atypical antipsychotics (clozapine, risperidone or olanzapine), one patient was taking both typical and atypical antipsychotics, and three patients were unmedicated.